

$\alpha$  decay of  $^{223}\text{Fr}$ : Level structure of  $^{219}\text{At}$ 

C. F. Liang and P. Paris

*Centre de Spectrométrie et de Spectrométrie de Masse, Bâtiment 104, F-91405 Campus Orsay, France*

R. K. Sheline

*Departments of Chemistry and Physics, Florida State University, Tallahassee, Florida 32306-4390*

(Received 24 October 2000; published 21 August 2001)

The  $\alpha$  decay of  $\alpha$  recoil collected sources of  $^{223}\text{Fr}$  was studied using a purified  $^{227}\text{Ac}$  source. Five  $\alpha$  groups were observed whereas previously only one was reported. Multipolarities and energies of the  $\gamma$  transitions between the  $^{219}\text{At}$  levels were observed for the first time which allowed spins and parities to be assigned to the levels. The systematics of the levels of  $^{215}\text{At}$ ,  $^{217}\text{At}$ , and  $^{219}\text{At}$  show a strong similarity, but with decreasing level energies with increasing mass. The levels in  $^{219}\text{At}$  are interpreted in terms of the shell model configurations  $\pi(h_{9/2})^3\nu(g_{9/2})^{-2}$  and  $\pi(h_{9/2})^2f_{7/2}\nu(g_{9/2})^{-2}$ . Although there is no evidence of parity doublets in  $^{215}\text{At}$ ,  $^{217}\text{At}$ , and  $^{219}\text{At}$ , some of their configurations are shown to be very closely related to the quadrupole-octupole deformed ground states of  $^{219}\text{Fr}$ ,  $^{221}\text{Fr}$ , and  $^{223}\text{Fr}$ , respectively.

DOI: 10.1103/PhysRevC.64.034310

PACS number(s): 27.80.+w, 27.90.+b, 21.60.Cs, 23.60.+e

## I. INTRODUCTION

Nothing is known about the  $\alpha$  decay of  $^{223}\text{Fr}$  except the existence of a single decaying  $\alpha$  with energy  $5340 \pm 80$  keV and with an  $\alpha$  branching ratio of  $6 \times 10^{-5}$  [1,2]. Obviously, a serious difficulty for further study is the extremely small branching ratio, so that no further reported studies have been undertaken in the past 44 years.

On the other hand, the structure of the daughter nucleus,  $^{219}\text{At}$ , is of considerable interest. It is well known that the region of nuclei with  $219 \leq A \leq 229$  can be understood in terms of quadrupole-octupole deformation. Indeed, the levels in the nucleus  $^{219}\text{Fr}$  have been interpreted in terms of quadrupole-octupole deformation [3], whereas the levels in the nucleus  $^{219}\text{Rn}$  have been interpreted as intermediate between quadrupole-octupole configurations and shell model configurations [4]. Conversely, the levels of  $^{215}\text{At}$  and  $^{217}\text{At}$  have only been described in terms of the shell model [5,6].

Because the nucleus  $^{219}\text{At}$  has such a large neutron excess, nuclear reaction methods are not available for its study. Therefore, in spite of the very small  $\alpha$  branching ratio of  $^{223}\text{Fr}$ , it is necessary to use this method of populating the levels in  $^{219}\text{At}$ .

Figure 1 is a schematic drawing of the nuclear relationships which must be taken into account in the process of studying the  $\alpha$  decay of  $^{223}\text{Fr}$  in order to observe the levels in  $^{219}\text{At}$ . Starting then with a pure  $^{223}\text{Fr}$  source obtained from  $^{227}\text{Ac}$   $\alpha$  recoils, one must still overcome the minuscule (0.02%)  $\alpha$  branching ratio of  $^{223}\text{Fr}$  observed in this research. This can be accomplished by collecting  $^{223}\text{Fr}$  recoils for 30 min and measuring the  $\alpha$  spectrum for 30 min, minimizing the buildup of  $^{223}\text{Ra}$ . The  $\alpha$  spectrum is then measured again after most of the  $^{223}\text{Fr}$  has decayed, leaving only the  $\alpha$  spectrum of  $^{223}\text{Ra}$  and its daughters. The different spectrum represents the  $^{223}\text{Fr}$  and the higher energy  $^{223}\text{Ra}$   $\alpha$  decays. The details of the experimental methods are given in the next section.

## II. EXPERIMENTAL METHODS AND RESULTS

We started with  $\sim 100 \mu\text{C}$  of  $^{227}\text{Ac}$  chemically purified from daughter activities from our initial  $^{227}\text{Ac}$  activity purchased from the Radiochemical Center, Amersham, England, several years ago. The solvent extraction method used involved a benzene (TTA) phase and an aqueous phase buffered at pH 5.7 [7]. Initially both the  $^{227}\text{Ac}$  and the  $^{227}\text{Th}$  were extracted into the benzene TTA phase. However, with a change of pH to 1.0 only the  $^{227}\text{Ac}$  returns to the aqueous phase. The  $^{227}\text{Ac}$  was evaporated to dryness and heated in vacuum at  $1800^\circ\text{C}$  onto a 0.1 mm Ta foil for use as an  $\alpha$  recoil source. About 3 h are required for this procedure. The  $^{223}\text{Fr}$  recoils from this  $^{227}\text{Ac}$  source impinged on a transport tape 2 mm away. The  $^{223}\text{Fr}$  recoils implanted in the tape were then moved between  $\alpha$  and  $\gamma$  detectors with a 30 min collec-

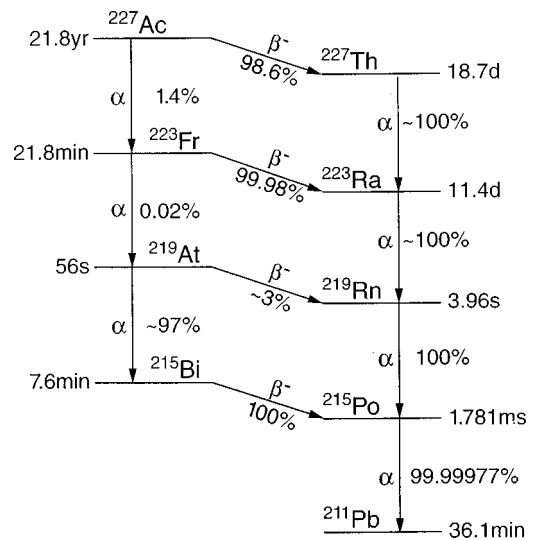


FIG. 1. Schematic drawing of the decay of  $^{227}\text{Ac}$  used as the primary source in this study. The large number of decay products (in addition to the  $^{223}\text{Fr}$  and  $^{219}\text{At}$  involved in this study) were serious impediments. The data for this figure are all taken from Ref. [10] except the  $\alpha/\beta$  branching which is from this study.

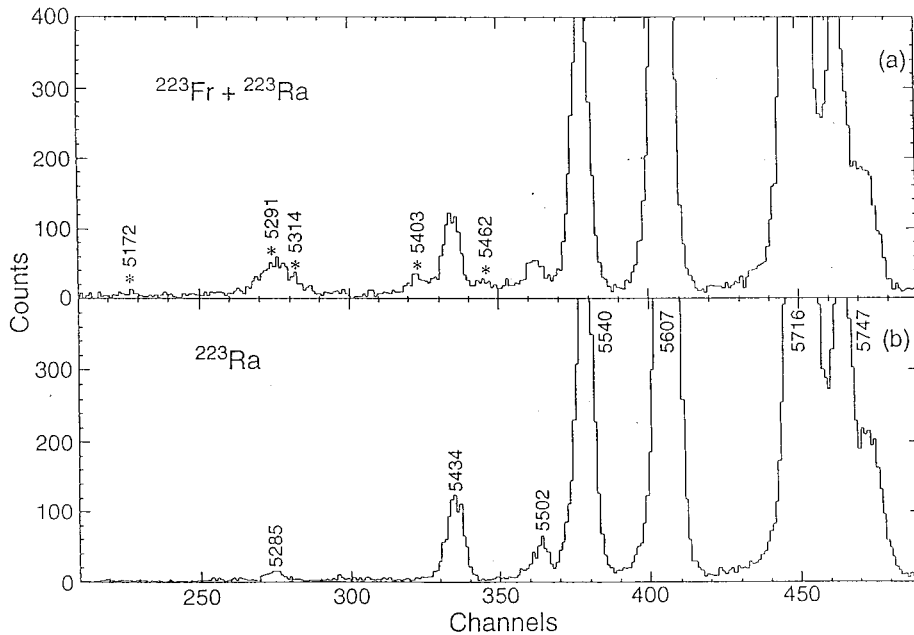


FIG. 2.  $\alpha$  spectra of  $^{223}\text{Fr}$  and  $^{223}\text{Ra}$ . (a) is the  $\alpha$  spectrum of a mixture of  $^{223}\text{Fr}$  and  $^{223}\text{Ra}$  obtained over a 10-h period from 20 sources.  $^{223}\text{Fr}$   $\alpha$ 's are labeled with an asterisk and with the energies of the  $\alpha$ 's in keV. (b) is the  $\alpha$  spectrum obtained in the same manner but with a 1-h delay. The  $^{223}\text{Ra}$   $\alpha$ 's are labeled with the energies in keV.

tion time and a 30 min measurement time, appropriate for the 21.8 min half-life of  $^{223}\text{Fr}$ .

The  $\alpha$  detector used in our measurements was an ion implanted Si wafer 200 mm<sup>2</sup> in area and 100  $\mu\text{m}$  thick with 17 keV resolution [full width at half maximum (FWHM)]. The  $\gamma$  detector was a 20% efficient coaxial Ge detector with a Be window sensitive to low energy  $\gamma$ 's [with 1 keV resolution (FWHM) at 100 keV]. The source was placed between  $\alpha$  and  $\gamma$  detectors in 180° very close geometry. The solid angles  $\Omega_\alpha$  and  $\Omega_\gamma$  were 15% and 10%, respectively. The Si  $\alpha$  detector was not sensitive to x rays ( $<0.1X_L$  and  $<0.01X_K$ ). The  $\alpha$ -X summing effect was less than 2%. Single  $\alpha$  and  $\gamma$  spectra with 512 channels for  $\alpha$  and 2048 channels for  $\gamma$  were taken together with  $\alpha$ - $\gamma$  coincidence measurements. Using this experimental setup two sets of studies have been undertaken.

#### A. Direct $\alpha$ and $\gamma$ measurements

Twenty sets of  $^{223}\text{Fr}$  recoils were collected on tape over a 10-h period using a freshly prepared  $^{227}\text{Ac}$  source. Each set was collected for 30 min and the  $\alpha$  spectra then measured for 30 min while the next set was being collected. The result is shown in Fig. 2(a). The large peaks correspond to  $^{223}\text{Ra}$   $\alpha$ 's, whereas the small peaks labeled with asterisks and with assigned energies in keV are presumably the  $\alpha$ 's of  $^{223}\text{Fr}$ . Figure 2(b) was obtained under identical conditions following the  $^{223}\text{Fr}$  measurement except that the measurement was started after a 1-h delay. The  $^{223}\text{Ra}$  results not only from the decay of  $^{223}\text{Fr}$ , as is true initially, but 20 h later the  $^{227}\text{Ac}$  source begins to build up  $^{227}\text{Th}$  which is a second source of  $^{223}\text{Ra}$  (see Fig. 1). This causes the  $^{223}\text{Fr}$   $\alpha$  peaks to be greatly reduced relative to the  $^{223}\text{Ra}$   $\alpha$  intensity. Comparison of Figs. 2(a) and 2(b) normalized for  $^{223}\text{Ra}$  intensity makes it quite clear that the five groups indicated with an asterisk in Fig. 2(a) have disappeared in Fig. 2(b) and are assigned as  $^{223}\text{Fr}$   $\alpha$ 's. The  $\alpha$  energies of  $^{223}\text{Ra}$  [4] were used for calibration of the  $^{223}\text{Fr}$   $\alpha$ 's. The 5291 plus 5314 keV  $\alpha$  group was mixed

with the 5285 keV  $\alpha$  of  $^{223}\text{Ra}$  which, however, can be subtracted quantitatively. Better information on the weak 5172 keV  $\alpha$  can be obtained from the coincidence study. Since the 5462 keV  $\alpha$  disappeared in the  $\gamma$ - $\alpha$  coincidence study it was assigned as populating the ground state of  $^{219}\text{At}$ .

Direct  $\gamma$  spectra were recorded simultaneously with the  $\alpha$  spectra and proved important in determining the  $\alpha/\beta^-$  branching ratio of  $^{223}\text{Fr}$ . In particular, the strong 50.1 keV  $\gamma$  in the  $^{223}\text{Ra}$  spectrum was used to deduce the accumulated activities of the  $^{223}\text{Fr}$  sources and from that we determine the  $\alpha$  branching. This is dealt with in the  $\alpha$  branching ratio section below.

#### B. $\alpha$ - $\gamma$ coincidence study

Using the same experimental setup after the direct  $\alpha$  and  $\gamma$  measurements,  $\alpha$ - $\gamma$  coincidence measurements were obtained from the  $^{223}\text{Fr}$  recoil sources over a period of 7 d. 30 min collection of activities followed by 30 min measurement cycles were used. The 1024  $\times$  1024 channel  $\alpha$ - $\gamma$  coincidence measurements were made with the  $^{223}\text{Fr}$  recoil sources between the  $\alpha$  and  $\gamma$  counters in 180° very close geometry. A second set of coincidence measurements was made with identical conditions, but with a  $^{223}\text{Ra}$  source to be used for subtractions. We found it necessary in order to have an accurate coincidence yield of the  $L$  x rays ( $X_L$ ) to increase the fast coincidence time to 400 ns instead of 150 ns generally used.

Figures 3, 4, and 5 show the  $\gamma$  spectra in coincidence with  $\alpha$  groups 5403, 5314+5291, and 5172 keV, respectively, which correspond to the excited levels of 60, 151, and 296 keV in  $^{219}\text{At}$ . In each of these three figures, the uppermost spectrum is that of  $\alpha$ - $\gamma$  coincidences from the  $^{223}\text{Fr}$  recoils extracted over a 7-d period. The middle spectrum is that from a  $^{223}\text{Ra}$  source under identical conditions and with an identical  $\alpha$  gate. The bottom spectrum is the difference between the upper two spectra, and therefore corresponds to the

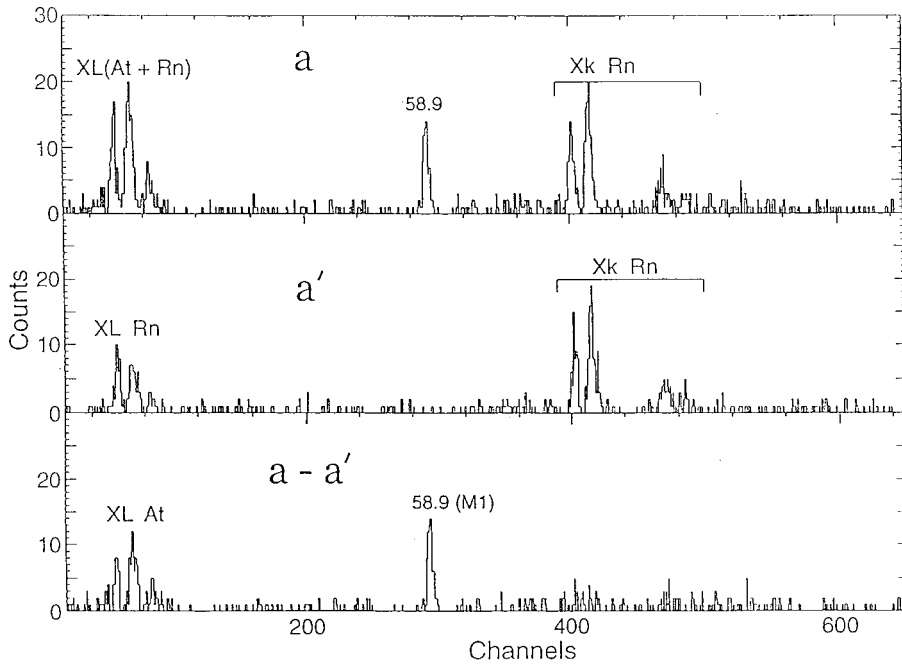


FIG. 3. The  $\gamma$  spectrum of  $^{219}\text{At}$  in coincidence with the 5403 keV  $\alpha$  of  $^{223}\text{Fr}$  taken over 7 d using 30 min cycles. The upper panel shows the  $\gamma$  spectrum from the  $^{223}\text{Fr}$  recoil sources; the middle panel under identical conditions, but with a  $^{223}\text{Ra}$  source. The lower panel shows the difference between the upper and middle panels. x rays are labeled and the  $\gamma$  ray is labeled in keV.

$\gamma$  spectrum in coincidence with the  $^{223}\text{Fr}$   $\alpha$ , excluding the contributions of  $^{223}\text{Ra}$ .

Figure 3 shows quite clearly the existence of a 58.9 keV  $\gamma$  in coincidence with the 5403 keV  $\alpha$ . The 58.9 keV energy corresponds almost exactly and well within experimental error with the  $Q_\alpha = E_\alpha + \text{recoil energy}$  difference between the two levels populated by the 5462 and 5403 keV  $\alpha$ 's. Finally, in Fig. 6, we gated on the 58.9 keV  $\gamma$  and observed only the 5403 keV  $\alpha$ .

Similarly, in Fig. 4, we found a 150.9 keV  $\gamma$  in coincidence with the broad  $\alpha$  group of 5291 + 5314 keV. The 150.9 keV fits very nicely with the  $Q_\alpha$  difference between the ex-

cited state populated by the 5314 keV  $\alpha$  and the ground state. When we gated on the 150.9 keV  $\gamma$  (Fig. 7) we observed three  $\alpha$  groups of 5314, 5291, and 5172 keV. This shows quite clearly the existence of transitions from 174 and 294 keV states to the 150.9 keV level.

In Fig. 5 we see evidence for the weak 145.3–150.9 keV  $\gamma$  cascade in coincidence with the 5172 keV  $\alpha$ . The 145.3 keV  $\gamma$  is about half the intensity of the 150.9 keV  $E2$   $\gamma$ .

Table I summarizes the electron conversion coefficient calculation from the ratio  $I_x(\text{At})/I_\gamma$  for the 58.9 and 150.9 keV  $\gamma$ 's. These intensities were extracted from the spectra ( $a-a'$ ) in Fig. 3 and ( $b-b'$ ) in Fig. 4. The efficiency of the

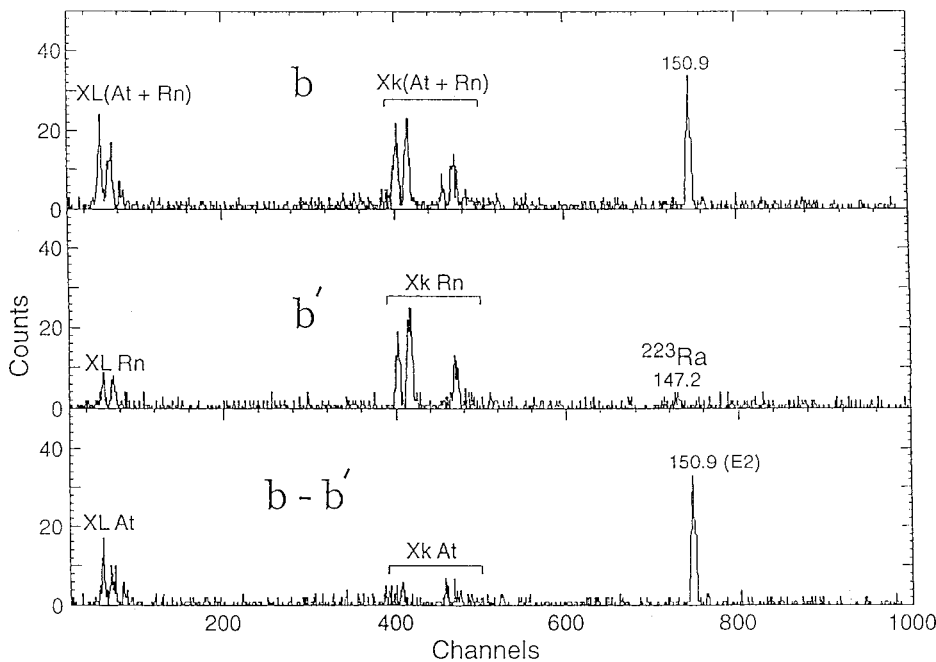


FIG. 4. The  $\gamma$  spectrum of  $^{219}\text{At}$  in coincidence with the 5291+5314 keV  $\alpha$ 's of  $^{223}\text{Fr}$  taken over 7 d using 30 min cycles. See Fig. 3 for the rest of the figure caption.

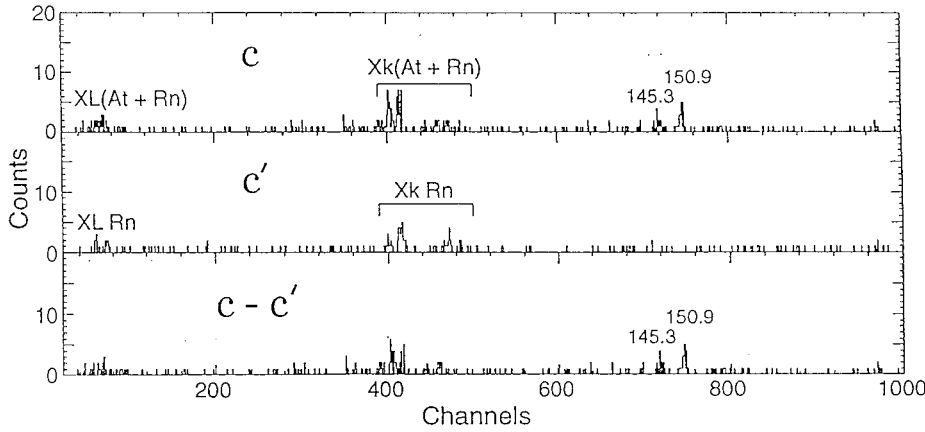


FIG. 5. The  $\gamma$  spectrum of  $^{219}\text{At}$  in coincidence with the 5172 keV  $\alpha$  of  $^{223}\text{Fr}$ . See Fig. 3 for the rest of the figure caption.

Ge detector was taken into account. The fluorescence yields  $\omega_L \cong 0.3$  is an average yield for the  $X_L$  group,  $\omega_K \cong 1$  for  $X_K$  [10]. The values in parentheses correspond to the errors which are significant due to the small intensities observed.

The  $\alpha_L$  conversion of the 58.9 keV  $\gamma$  ( $7.2 \pm 3.5$ ) is compatible with an  $M1$  transition; a few percent of  $E2$  mixing is not excluded. For the 150.9 keV  $\gamma$ , only an  $E2$  multipolarity satisfies both the  $\alpha_L$  and  $\alpha_K$  conversion coefficients.

In Fig. 5 we see evidence for a weak 145.3–150.9 keV  $\gamma$  cascade in coincidence with the 5172 keV  $\alpha$  which populates the 296 keV level. The lower panel ( $c-c'$ ) of Fig. 5 shows these two  $\gamma$ 's with intensities  $I_{\gamma 145}/I_{\gamma 151} = 0.5 \pm 0.2$ . If we assume the 150.9 keV gamma has  $E2$  multipolarity as suggested above and the intensity  $\gamma(1 + \alpha_{\text{tot}})$  is conserved in the cascade, we deduced an  $\alpha_{\text{tot}} = 5 \pm 2$  for the 145.3 keV  $\gamma$ . Comparing with the theoretical  $\alpha_{\text{tot}}$  values ( $E1$  0.16,  $M1$  4.0,  $E2$  1.6) an  $M1$  multipolarity with some possible  $E2$  mixing is proposed for the 145.3 keV transition.

### C. $\alpha$ - $\beta$ branching evaluation in $^{223}\text{Fr}$

In Sec. II A, the direct  $\gamma$  measurement of the intensity of the 50.1 keV  $\gamma$  from the  $^{223}\text{Fr} \rightarrow ^{223}\text{Ra}$   $\beta$  decay [ $I_\gamma = (36$

$\pm 7)\% \beta$  [10]] was determined at the same time as the  $\alpha$  intensities of Fig. 2(a) were measured. If we now know the relative solid angle between the  $\alpha$  and  $\gamma$  detectors we can deduce this  $\alpha$ - $\beta$  branching ratio. For this purpose we evaporated a thin  $^{227}\text{Th}$   $\alpha$  source on thin Al foil and placed this source in the exact location in which the  $^{223}\text{Fr}$  sources had been placed. Direct  $\alpha$  and  $\gamma$  spectra of  $^{227}\text{Th}$  were recorded, giving an  $\alpha$  to 50.1 keV  $\gamma$  intensity ratio which was used with the known  $I_\gamma(50.1) = (8 \pm 1)\% \alpha$  [10] to calculate the normalization factor  $k = (2.7 \pm 1.1) \times 10^{-7}$ . Using this factor we change the  $\alpha$  measured intensities to  $\alpha$ - $\beta$  branching.

Table II summarizes the  $\alpha$  energies and  $\alpha$  branching in the  $^{223}\text{Fr} \rightarrow ^{219}\text{At}$  decay. The  $\alpha$  hindrance factors (HF) (column 4) were calculated with the classic formula,

$$(\log_{10} T_{1/2})_{\text{theo}} = A + BQ^{-1/2}.$$

$A$  and  $B$  were deduced with the two strong  $\alpha$  transitions in the neighboring  $^{221}\text{Fr}$  isotope [6]:

$E_\alpha = 6340$ keV	83.4%	HF=3.8
$= 6125$ keV	15.1%	HF=2.4.

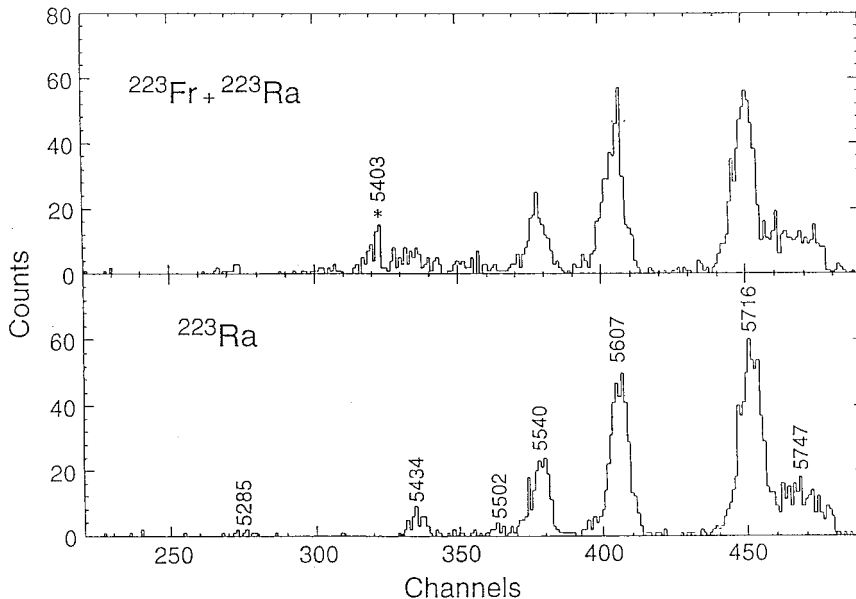


FIG. 6.  $\alpha$  spectra of  $^{223}\text{Fr}$  and  $^{223}\text{Ra}$  in coincidence with the 58.9 keV  $\gamma$  of Fig. 3. The 5403 keV  $\alpha$  of  $^{223}\text{Fr}$  is labeled both with an asterisk and its energy in the upper panel. The  $\alpha$ 's of a pure  $^{223}\text{Ra}$  source are labeled with their energies in keV in the lower panel.

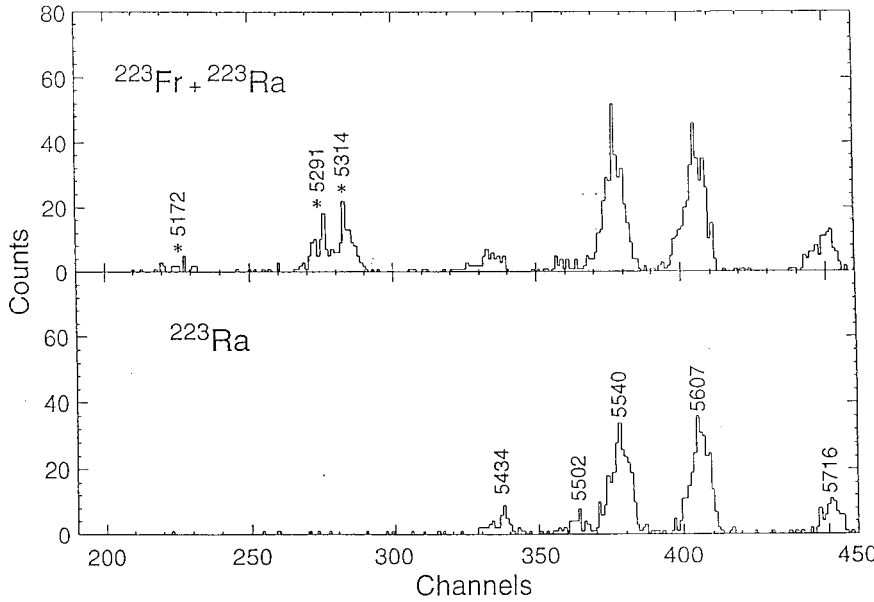


FIG. 7.  $\alpha$  spectra of  $^{223}\text{Fr}$  and  $^{223}\text{Ra}$  in coincidence with the 150.9 keV gamma of Fig. 4. The  $^{223}\text{Fr}$   $\alpha$ 's are labeled with asterisks and energies in keV in the upper panel.  $^{223}\text{Ra}$   $\alpha$ 's are labeled in the lower panel.

The comparison of the observed partial half-life with the calculated half-life gives us HF directly.

The  $\alpha$  feeding and the  $(\gamma+e)$  intensities balance are given in Table III. It should also be noted that although we have not observed explicitly the  $\sim 23$  keV  $\gamma$  between the  $\sim 174$  and 150.9 keV levels, the  $\alpha$  feeding to the  $\sim 174$  keV level is necessary to have the correct intensity balance for the 150.9 keV  $\gamma$  transition. Finally, there was no incompatibility between the  $\alpha$  feeding and  $(\gamma+e)$  intensities out using the multipolarities deduced above.

### III. LEVEL SCHEME OF $^{219}\text{At}$

Using the results from Figs. 2–7 and Tables I–III, the level scheme to the right in Fig. 8 is proposed for  $^{219}\text{At}$ . It contains all five  $\alpha$  transitions and three  $\gamma$  transitions explicitly observed, and one which is inferred. The level structure including the transitions between states is quite firm. Furthermore, the parities of all states have been determined as negative and the spins of four of the five states are reasonably certain. Specifically, the  $3/2^-$   $J^\pi$  values of the 296 and  $\sim 174$  keV states are assigned as a result of the very low hindrance factors (two in each case) of the  $\alpha$  decay from the known  $3/2^-$  ground state of  $^{223}\text{Fr}$  [7,8]. The  $9/2^-$   $J^\pi$  value of the ground state is strongly suggested by the systematics

of the  $9/2^-$  ground state values in  $^{215}\text{At}$  and  $^{217}\text{At}$  (Fig. 8). It is also suggested by the low hindrance factor of the alpha decay of  $^{219}\text{At}$  to  $^{215}\text{Bi}$  (1.9) which must be presumed to have  $J^\pi=9/2^-$  [9] in view of its strong population of the  $11/2^+$  state in  $^{215}\text{Po}$  in  $\beta^-$  decay and its much lower population of the  $5/2^+$  state. The  $5/2^-$  assignment for the 150.9 keV state then follows naturally from the 145 keV  $M1-151$  keV  $E2$  cascade. The  $7/2^-$  assignment for the 58.9 keV state is consistent also with the  $^{215}\text{At}$  and  $^{217}\text{At}$  systematics and consistent also with the  $M1$  transition of the  $9/2^-$  ground state. However, because of the uncertainties, we have enclosed this spin in parentheses.

### IV. DISCUSSION

#### A. Shell model configurations in $^{219}\text{At}$

Presumably the  $9/2^-$  ground state in  $^{219}\text{At}$  results from the coupling of three  $h_{9/2}$  protons beyond the 82 proton closed shell to a  $J^\pi$  of  $9/2^-$ , and the coupling of the eight  $g_{9/2}$  neutrons beyond the 126 neutron shell to a  $J^\pi$  of  $0^+$ . Then the ground state configuration of  $^{219}\text{At}$  is  $\{\pi(h_{9/2})^3\nu(g_{9/2})^{-2}\}_{9/2^-}$ .

The next configuration expected from the shell model should be  $f_{7/2}$  as experimentally observed in  $^{209}\text{Bi}$  and in

TABLE I. Electron conversion  $\alpha_L$  and  $\alpha_K$  calculation for 58.9 and 150.9 keV  $\gamma$ 's.

$E_\gamma$ (keV)	$\alpha_L = \frac{I_L}{I_\gamma \bar{\omega}} \bar{\omega} \approx 0.3$	$\alpha_L$ Theor.	Assign.	$\alpha_K = \frac{I_K}{I_\gamma \omega_K} \omega_K \approx 1$	$\alpha_K$ Theor.	Assign.
58.9	$\frac{130(30)}{68(20) \times 0.3} = 7.2(3.5)$	$E1$ 0.3 $M1$ 8.8 $E2$ 72.0	$M1$			
150.9	$\frac{98(30)}{252(25) \times 0.3} = 1.4(0.6)$	$E1$ 0.03 $M1$ 0.56 $E2$ 0.85	$M1, E2$	$\frac{50(22)}{252(25)} = 0.22 \pm 0.11$	$E1$ 0.13 $M1$ 3.2 $E2$ 0.29	$E1, E2$

TABLE II.  $\alpha$  energies, measured and normalized intensities.

$E_\alpha$ (keV)	$I_\alpha$ (measured)	$I_\alpha(10^{-6}\beta) = kI_\alpha^a$	HF
5462 (3)	137 (25)	40 (20)	30 (15)
5403 (3)	182 (30)	50 (20)	10 (4)
5314 (4)	220 (30)	60 (30)	3 (1.5)
5291 (4)	250 (30)	70 (30)	2 (1)
5172 (5)	39 (15)	$\sim 10$	$\sim 2$

<sup>a</sup>The  $\alpha$  intensities are in units of  $10^{-6}$   $\beta$  particles with  $K=(2.4 \pm 1.0) \times 10^{-7}$  as described in the text.

both <sup>215</sup>At and <sup>217</sup>At. This is the state at 58.9 keV in <sup>219</sup>At and is assigned the complete configuration  $\{\pi(h_{9/2})^2 f_{7/2} \nu(g_{9/2})^{-2}\}_{7/2^-}$ .

The  $5/2^-$  150.9 keV,  $3/2^-$   $\sim 174$  keV, and  $3/2^-$  296 keV states in <sup>219</sup>At may be parts of the seniority three proton configurations:  $(h_{9/2})^3$  and  $(h_{9/2})^2 f_{7/2}$  as observed in both <sup>215</sup>At and <sup>217</sup>At. Unfortunately, many of the expected states of these seniority three configurations are not observed in <sup>219</sup>At. It is therefore necessary to rely heavily on the more complete level structures in <sup>217</sup>At and <sup>215</sup>At and draw analogies with <sup>219</sup>At. This is done in Fig. 8 as implied by the dashed lines. Since the  $3/2^-$  368 keV and  $5/2^-$  218 keV states in <sup>217</sup>At are parts of the seniority three  $(f_{7/2})^3$  proton configurations, by analogy we believe  $3/2^-$  296 keV and  $5/2^-$  150.9 keV states in <sup>219</sup>At are parts of this configuration (Fig. 8). Assuming this is correct, it is interesting that the 145.3–150.9 keV cascade also implies a relatedness in the  $(f_{7/2})^3$  proton configuration. In a similar way the  $3/2^-$   $\sim 174$  keV state in <sup>219</sup>At, by analogy with the  $3/2^-$  state at 271.8 keV in <sup>217</sup>At, becomes a part of the seniority three  $(h_{9/2})^2 f_{7/2}$  proton configuration.

### B. Comparison of the level structures of <sup>215</sup>At, <sup>217</sup>At, and <sup>219</sup>At

Figure 8 presents a comparison between the level structures of <sup>215</sup>At [5], <sup>217</sup>At [6], and <sup>219</sup>At observed in this study. The similarities are obvious. This is however expected in view of the fact that the ground state configuration is  $\pi(h_{9/2})^3 \nu(g_{9/2})^n$  for each of the three nuclei. Furthermore, the first excited configuration in each of the three nuclei is  $\pi(h_{9/2})^2 f_{7/2} \nu(g_{9/2})^n$ . The excitation energies decrease as we go through the sequence <sup>215</sup>At–<sup>217</sup>At–<sup>219</sup>At. This results from the higher core energies in <sup>214</sup>Po and <sup>216</sup>Rn (an average of 537 keV) compared to <sup>216</sup>Po and <sup>218</sup>Rn (an average of 437

TABLE III.  $\alpha$  and  $(\gamma + e^-)$  intensity balance.

$E_\gamma$ (keV)	$I_\gamma^a$	$I_\gamma(1 - \alpha_{tot})^a$	$\alpha$ feeding <sup>a</sup>	Conclusion
58.9 (2)	8 (3)	$M1$ 95 (35) $E2$ 870 (300)	50 (20)	$M1$
150.9 (2)	56 (5)	$M1$ 280 (25) $E2$ 140 (12)	140 (50)	$E2 + (M1)$
145.3 (3)	2 (1)	$M1$ 10 (5) $E2$ 5 (2)	10 (5)	$M1 + (E2)$

<sup>a</sup>The  $\gamma$  and  $\alpha$  intensities are in units of  $10^{-6}$   $\beta$  particles.

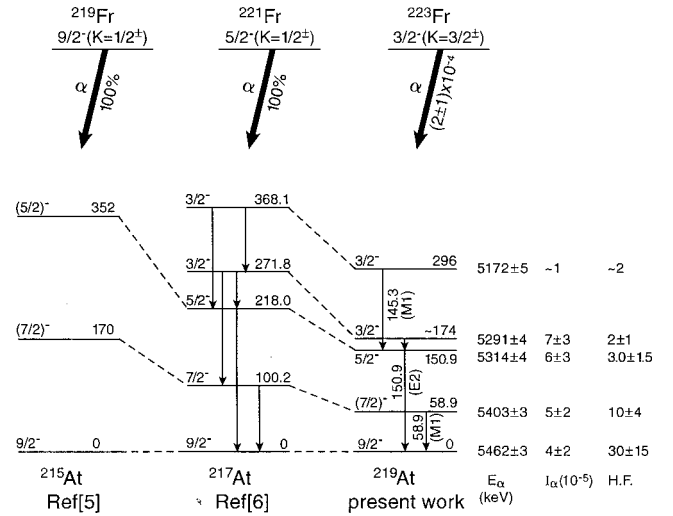


FIG. 8. Level scheme of <sup>219</sup>At as observed in the  $\alpha$  decay of <sup>223</sup>Fr and comparison with partial level schemes of <sup>217</sup>At and <sup>215</sup>At. To the right the level scheme of <sup>219</sup>At observed in this study is presented along with the energies in keV, the intensities and the hindrance factors (HF) of the  $\alpha$ 's populating the levels. Vertical lines indicate  $\gamma$  transitions which are labeled with energies in keV, and multiplicities. Shell model configurations are discussed in the text. Dashed lines connect related levels in the three At isotopes. The  $K$  values of the  $\alpha$  decaying Fr isotopes, as observed in the literature [3,7,8,11], are also indicated because of their importance in establishing relationships with the At daughters.

keV) compared to <sup>218</sup>Po and <sup>220</sup>Rn (an average of 376 keV) [10]. Indeed, there is a drastic difference in the energies <sup>218</sup>Po (511 keV) and <sup>220</sup>Rn (241 keV) indicative of a sudden increase in collectivity in the region of <sup>219</sup>At. The difference in energy between the seniority three states in <sup>219</sup>At (150.9 and 296 keV), an average of 223.5 keV, and the seniority one ground state suggests that <sup>219</sup>At is more collective than either the <sup>218</sup>Po or <sup>220</sup>Rn cores.

### C. Relationship of <sup>215</sup>At, <sup>217</sup>At, and <sup>219</sup>At to the quadrupole-octupole collective model

There is no evidence in <sup>215</sup>At, <sup>217</sup>At, or <sup>219</sup>At for parity doublet bands and their associated very fast  $E1$  transitions and decoupling parameters for  $K=1/2^\pm$  bands with similar absolute values but opposite signs. This would suggest that there is no evidence in these nuclei for quadrupole-octupole deformation. However, we wish to suggest that hindrance factors in  $\alpha$  decay of <sup>219</sup>Fr, <sup>221</sup>Fr, and <sup>223</sup>Fr represent evidence of a relationship between these nuclei with known  $K$  values and quadrupole-octupole collectivity [3,7,8,11] and the daughters <sup>215</sup>At, <sup>217</sup>At, and <sup>219</sup>At.

Specifically, the  $9/2^-$  ground state of <sup>219</sup>Fr has been shown [3] to be the anomalous member of the  $1/2^- (-0.1 -0.5 -2)$  quadrupole-octupole deformed orbital which at  $\epsilon_3 = \epsilon_2 = 0$  goes over into the  $h_{9/2}$  shell model orbital. For a more detailed description of the quadrupole-octupole deformed model, see Ref. [3]. In  $\alpha$  decay the <sup>219</sup>Fr ground state populates the  $9/2^-$  ground state of <sup>215</sup>Ac with hindrance factor 1.2 [5]. Low hindrance factors are also ob-

served in the population in the  $\alpha$  decay of the seniority three  $(h_{9/2})^3$  proton configuration, in contrast to the high hindrance factor (130) in populating the  $(h_{9/2})^2 f_{7/2}$  state in  $^{215}\text{At}$ . A very similar statement can be made for the  $\alpha$  decay of  $^{221}\text{Fr}$  into  $^{217}\text{At}$  [6]. In this case, because of the somewhat smaller decoupling parameter, the  $5/2^-$  member of the  $1/2^-$  ( $-0.1$   $-0.5$   $-2$ ) quadrupole-octupole deformed orbital is the ground state [11] and  $\alpha$  decays with low hindrance factors to the  $9/2^-$  ground state (3.8) and with the seniority three members of the  $(h_{9/2})^3$  proton configuration. Again, the hindrance factor to the  $(h_{9/2})^2 f_{7/2}$  state is much higher (87).

However, the  $\alpha$  decay of  $^{223}\text{Fr}$  into  $^{219}\text{At}$  is quite different. The  $3/2^-$  ground state of  $^{223}\text{Fr}$  results from the  $3/2^-$  (0.1 0) quadrupole-octupole deformed orbital [7] which at  $\epsilon_3 = \epsilon_2 = 0$  goes over into the  $f_{7/2}$  shell model orbital. However, this orbital is highly mixed with the  $1/2^-$  ( $-0.2$   $-0.5$   $-2$ ) orbital which produced the ground states of  $^{219}\text{Fr}$  and  $^{221}\text{Fr}$ . We observe [7] this mixing in the band structure of the  $K^\pi = 3/2^-$  band which takes on a considerable amount of the anomalous structure of the  $K^\pi = 1/2^-$  band. In the  $\alpha$  decay of  $^{223}\text{Fr}$  presented in this paper the hindrance factors to all of the states populated are quite small. The smallest are to the two  $3/2^-$  states, but none of the hindrance factors is  $>30$ . This is indicative of the mixing which allows population of both the  $(h_{9/2})^3$  and  $(h_{9/2})^2 f_{7/2}$  configurations in  $^{219}\text{At}$ .

Taken together, all of this  $\alpha$  decay evidence indicates that, although we see no parity doublets in  $^{215}\text{At}$ ,  $^{217}\text{At}$ , and  $^{219}\text{At}$ , some of the configurations are clearly closely related

to the quadrupole-octupole deformed ground states of the  $\alpha$  decaying parents.

## V. CONCLUSIONS

In spite of the extremely small  $\alpha/\beta^-$  branching of  $^{223}\text{Fr}$  we were still able to observe five  $\alpha$  groups populating the ground state and four excited states in  $^{219}\text{At}$ . The only previous study of the  $\alpha$  decay [1,2] suggested a single  $\alpha$  populating a level(s) in the middle of the excitation region according to the present studies. Multipolarities of the  $\gamma$  transitions between the five states allowed us to determine definite spin-parities for four of the five states. The systematics of the energies of the states in  $^{215}\text{At}$ ,  $^{217}\text{At}$ , and  $^{219}\text{At}$  were compared and similarities were obvious with the spacing between the  $\pi(h_{9/2})^3 \nu(g_{9/2})^n$  and  $\pi(h_{9/2})^2 f_{7/2} \nu(g_{9/2})^n$  decreasing in this sequence. Although there was no evidence of parity doublets and associated expectations, we were able to show that some of the configurations in  $^{215}\text{At}$ ,  $^{217}\text{At}$ , and  $^{219}\text{At}$  were closely related to the quadrupole-octupole deformed ground state configurations in  $^{219}\text{Fr}$ ,  $^{221}\text{Fr}$ , and  $^{223}\text{Fr}$ .

## ACKNOWLEDGMENTS

This research has been supported by the State of Florida. One of us (R.K.S.) also wishes to thank CSNSM and IPN at Université de Paris-Sud, Campus Orsay, for hospitality on a variety of occasions.

- 
- [1] M. J. P. Adloff, *Compt. Rend.* **240**, 1421 (1955).  
 [2] M. Perrey and M. J. P. Adloff, *J. Phys. Radium* **17**, 545 (1956).  
 [3] C. F. Liang, P. Paris, J. Kvasil, and R. K. Sheline, *Phys. Rev. C* **44**, 676 (1991).  
 [4] R. K. Sheline, C. F. Liang, and P. Paris, *Phys. Rev. C* **57**, 104 (1998).  
 [5] C. F. Liang, P. Paris, and R. K. Sheline, *Phys. Rev. C* **47**, 1801 (1993).  
 [6] R. K. Sheline, C. F. Liang, and P. Paris, *Phys. Rev. C* **51**, 1192 (1995).  
 [7] R. K. Sheline, C. F. Liang, P. Paris, J. Kvasil, and D. Nosek, *Phys. Rev. C* **51**, 1708 (1995).  
 [8] W. Kurcewicz, G. Løvghøiden, T. F. Thorsteinsen, M. J. G. Borge, M. Cronqvist, H. Gabelmann, H. Gietz, P. Hill, N. Kafrell, R. A. Naumann, K. Nybø, G. Nyman, J. Rogowski, and the ISOLDE Collaboration, *Nucl. Phys.* **A539**, 451 (1992).  
 [9] E. Ruchowska, J. Zylicz, C. F. Liang, P. Paris, and Ch. Briançon, *J. Phys. G* **16**, 255 (1990).  
 [10] R. B. Firestone and V. S. Shirley, *Table of Isotopes*, 8th ed. (Wiley, New York, 1996).  
 [11] R. K. Sheline, *Phys. Lett. B* **205**, 11 (1988); C. F. Liang, A. Peghaire, and R. K. Sheline, *Mod. Phys. Lett. A* **5**, 1243 (1990).